

1 **Type of Paper:** Original research article

2

3 **Title:** Visualization of root extracellular traps in an ectomycorrhizal woody plant (*Pinus*  
4 *densiflora*) and their interactions with root-associated bacteria

5

6 **Authors:** Makoto Shirakawa\*,<sup>1,2</sup>, Norihisa Matsushita<sup>1</sup>, Kenji Fukuda<sup>1</sup>

7

8 **Affiliations:**

9 **1:** Graduate School of Agricultural and Life Sciences, The University of Tokyo, 1-1-1 Yayoi,  
10 Bunkyo-ku, Tokyo, 113-8657, Japan

11 **2:** Research Fellow of Japan Society for the Promotion of Science (DC)

12

13 **•:** corresponding author

14 **E-mail:** mshirakawa941@g.ecc.u-tokyo.ac.jp (mk.shirakawa@gmail.com)

15 **Orcid-ID:** 0000-0003-3454-6768

16

17 **Main Conclusion:** Extracellular traps in the primary root of *Pinus densiflora* contribute to root-  
18 associated bacterial colonization. Trapped rhizobacteria induce the production of reactive oxygen  
19 species in root-associated, cap-derived cells.

20

21 **Abstract**

22 Ectomycorrhizal (ECM) woody plants, such as members of Pinaceae and Fagaceae, can acquire  
23 resistance to biotic and abiotic stresses through the formation of mycorrhiza with ECM fungi.

24 However, germinated tree seedlings do not have mycorrhizae and it takes several weeks for  
25 ectomycorrhizae to form on their root tips. Therefore, to confer protection during the early

26 growth stage, bare primary roots require defense mechanisms other than mycorrhization. Here,

27 we attempted to visualize root extracellular traps (RETs), an innate root defense mechanism, in

28 the primary root of *Pinus densiflora* and investigate the interactions with root-associated bacteria

29 isolated from ECM and fine non-mycorrhizal roots. Histological and histochemical imaging and

30 colony forming unit assays demonstrated that RETs in *P. densiflora*, mainly consisting of root-

31 associated, cap-derived cells (AC-DCs) and large amounts of root mucilage, promoted bacterial

32 colonization in the rhizosphere, despite also having bactericidal activity via extracellular DNA.

33 Four rhizobacterial strains induced the production of reactive oxygen species (ROS) from host  
34 tree AC-DCs without being excluded from the rhizosphere of *P. densiflora*. In particular,  
35 applying two *Paraburkholderia* strains, PM O-EM8 and PF T-NM22, showed significant  
36 differences in the ROS levels from the control group. These results reveal an indirect  
37 contribution of rhizobacteria to host root defense, and suggest that root-associated bacteria could  
38 be a component of RETs as a first line of defense against root pathogens in the early growth  
39 stage of ECM woody plants.

40

41 **Keywords:**

42 Border cells; Japanese red pine; *Paraburkholderia*; Primary root; Rhizobacteria; Root mucilage

43

44 **Abbreviations**

45 **AC-DCs:** root-associated, cap-derived cells, **CFU:** colony-forming unit, **CV:** crystal violet,

46 **CW:** calcofluor white, **exDNA:** extracellular DNA, **RAM:** root apical meristem, **RBC:** root

47 border cell, **RBLC:** root border-like cell, **RETs:** root extracellular traps, **ROS:** reactive oxygen

48 species

## 49 **Introduction**

50 Plants have root apical meristems (RAMs) on the root tip, which is a vital organ that controls  
51 cellular division and differentiation (Motte et al. 2019). Roots are constantly exposed to various  
52 biotic and abiotic stresses during elongation through soil (Cramer et al. 2011; Suzuki et al. 2014;  
53 Ganesh et al. 2022). Among stressors, pathogen attack is a major cause of mortality of juvenile  
54 plants (Atkinson and Urwin 2012; Gonthier and Nicolotti 2013). Plants repel or mitigate  
55 pathogen invasion and infection via innate defense responses, such as pathogen/microbe-  
56 associated molecular pattern (PAMP/MAMP)-triggered immunity (Huot et al. 2014; Cook et al.  
57 2015). Furthermore, numerous studies have shown that host roots recruit nonpathogenic, root-  
58 associated bacteria by releasing various root exudates (Badri and Vivanco 2009; Sasse et al.  
59 2018). Such bacteria produce exopolysaccharides, antipathogenic metabolites, and  
60 phytohormones, which in turn help control the rhizosphere environment (De Vleeschauwer and  
61 Höfte 2009; Kuzyakov and Razavi 2019; Mohanram and Kumar 2019). With the development of  
62 high-throughput sequencing technologies, we have come to better understand the interactions  
63 between host plants and pathogenic, commensal, and mutualistic rhizospheric microorganisms,  
64 as well as their impacts on the health and productivity of host plants.

65 Rhizodeposits include water-soluble and volatile compounds that are released from host roots,  
66 and are involved in biological defense. The root cap is made up of root border cells (RBCs) and  
67 root border-like cells (RBLCs), which cover vital tissues and release single or connected cells  
68 into the soil. Collectively, RBCs and RBLCs are termed root-associated, cap-derived cells (AC-  
69 DCs) (Hawes and Lin 1990; Hawes et al. 2003; Driouich et al. 2019). Studies have revealed that  
70 these cells remain alive after release from the root cap (Hawse and Pueppke 1986) and secrete  
71 mucilage composed of a mixture of polysaccharides, proteoglycans, extracellular DNA  
72 (exDNA), defensin peptides, reactive oxygen species (ROS), and various secondary metabolites  
73 (Plancot et al. 2013; Wen et al. 2017; Driouich et al. 2019; Driouich et al. 2021). These

74 structures, consisting of AC-DCs and their secretions that spread to encompass the root cap, are  
75 known as root extracellular traps (RETs) because of similarities with neutrophil extracellular  
76 traps, which are part of the innate immune system in animals (Brinkmann et al. 2004; Driouich et  
77 al. 2013). Studies on RETs have mainly focused on their defense functions against root  
78 pathogens. Most studies have used herbaceous plant species, such as *Arabidopsis* (*Arabidopsis*  
79 *thaliana* [L.] Heynh), cotton (*Gossypium* spp.), maize (*Zea mays* L.), and pea (*Pisum sativum* L.)  
80 (Hawes et al. 2003; Vicré et al. 2005; Wen et al. 2009; Hawes et al. 2016; Fortier et al. 2023). By  
81 contrast, the roles of RETs in woody plants remain poorly understood, and only a few cases have  
82 been investigated, including in *Acacia mangium* Willd. (Endo et al. 2011), grapevine (*Vitis*  
83 *riparia* × *Vitis labrusca*) (Liu et al. 2019), and some species in arid regions (*Balanites*  
84 *aegyptiaca* [L.] Del. fruits, *Acacia raddiana* Savi, and *Tamarindus indica* L.) (Carreras et al.  
85 2020).

86 Pinaceae is a representative ectomycorrhizal (ECM) tree family that inhabits temperate and  
87 boreal forests in the Northern Hemisphere. This family acquires resistance to biotic and abiotic  
88 stresses, including pathogen attacks, via belowground ECM associations. Such resistance allows  
89 Pinaceae species to invade non-forested sites and survive in the seedling stage (Martín-Pinto et  
90 al. 2006; Zhang et al. 2017; Policelli et al. 2019). However, ECM fungi generally associate with  
91 only fine root tips ( $\leq 2$  mm in diameter), which generate from lateral roots. This suggests that  
92 there is a period between seed germination and ECM root formation of weakened defense  
93 responses during root formation. Therefore, we hypothesized that other defense mechanisms  
94 confer protection in the early growth stage, and focused our investigations on RETs and root-  
95 associated bacteria.

96 We elucidated the features and roles of RETs in the early stage of germination of ECM tree  
97 species. To this end, we visualized the RETs of an ECM woody gymnosperm, Japanese red pine  
98 (*Pinus densiflora* Sieb. et Zucc.), investigated whether RETs in the host tree species for early

99 growth kill root-associated bacteria or promote their colonization, and evaluated the effects of  
100 those bacteria on the defense responses of host tree AC-DCs.

101

## 102 **Materials and Methods**

### 103 **Plant material**

104 *Pinus densiflora* seeds were immersed in distilled water in darkness at 4°C overnight (for 12–  
105 18 h). They were shaken in a neutral detergent solution for 1 min using a magnetic stirrer and  
106 rinsed with tap water. Intact seeds were surface sterilized with 30% (v/v) hydrogen peroxide for  
107 30 min and rinsed several times with sterile water; then they were sown on sterile filter paper  
108 moistened with sterile water and incubated under aseptic conditions in darkness at 25°C for 4–14  
109 days (mainly those germinated on the fourth or fifth day of culture with a root length < 2 cm  
110 were used). Before separation of RETs from the root cap for microscopic observation or  
111 experimentation, germinated seeds were soaked on sterile filter paper soaked with sterile water  
112 and incubated overnight under the same conditions as described above. Hereafter, this process is  
113 referred to as the swelling treatment (Fig. 1a, b).

114

### 115 **Isolation and identification of rhizobacterial strains**

116 Table 1 lists the four bacterial strains used in this study. To obtain rhizobacteria, we collected  
117 root system samples of mature *P. densiflora* trees in August 2020 at Ome Forest, a temperate  
118 secondary forest in Ome, Tokyo, Japan (35°47'50.4"N, 139°15'44.4"E), and the University of  
119 Tokyo Tanashi Forest, a planted forest in Nishitokyo, Tokyo, Japan (35°44'21"N, 139°32'15"E).  
120 The samples were gently washed in tap water with a brush under a stereomicroscope (Leica  
121 MZ16; Leica Microsystems, Wetzlar, Germany). Five ECM root tips of the same morphotypes  
122 and the same number of non-mycorrhizal (NM) root tips were selected from each sample. They  
123 were transferred to a 1.5 mL tube containing 1 mL sterile water and shaken for 1 min using a

124 vortex to remove fine particles. After repeating this process three times, each root tip was  
125 homogenized using a micropestle and suspended in 1 mL sterile water. The suspension was used  
126 as a stock solution, which was serially diluted up to 10,000 times, and 100  $\mu$ L each dilution was  
127 spread on yeast glucose (YG) agar medium containing 1.0 g yeast extract, 1.0 g glucose, 0.3 g  
128  $K_2HPO_4$ , 0.3 g  $KH_2PO_4$ , 0.2 g  $MgSO_4 \cdot 7H_2O$ , 15 g agar, and 1 L distilled water. All medium  
129 plates were incubated in darkness at 25°C for 2–7 days, and bacterial colonies generated on the  
130 plate were randomly isolated, of which four strains with different colony morphologies were  
131 selected for this study.

132 Species identification of the four bacterial strains was based on the 16S ribosomal RNA  
133 (rRNA) gene sequence. The V1–V9 regions of the 16S rRNA genes were amplified by direct  
134 polymerase chain reaction (PCR) from a single colony using EmeraldAmp PCR Master Mix  
135 (Takara Bio, Shiga, Japan), and the universal primer pair 27F and 1492R (Weisburg et al. 1991).  
136 The PCR cycling conditions were as follows: denaturing at 94°C for 1 min; 40 cycles of 98°C for  
137 10 s, annealing at 55°C for 30 s, and 72°C for 90 s; and a final extension at 72°C for 7 min.  
138 Successfully amplified PCR products were purified using illustra ExoProStar (GE Healthcare,  
139 Buckinghamshire, UK) and submitted to MacroGen DNA Sequencing Service (MacroGen,  
140 Tokyo, Japan) for Sanger sequencing. Four universal primers (27F, 518F, 800R, and 1492R)  
141 were used as sequencing primers to obtain nearly complete sequences (>1300 bp). After  
142 checking the quality check of the obtained sequences with reference to the original  
143 chromatograms, bacterial species were identified at least to the genus level via a BLAST search  
144 of the GenBank database (<http://blast.ncbi.nlm.nih.gov/Blast.cgi>). These sequences were  
145 deposited in the DNA Database of Japan (<https://www.ddbj.nig.ac.jp/index-e.html>) under the  
146 accession numbers LC743733–LC743736.

147

#### 148 **Histochemical staining and microscopy of RETs**

149 Root tips from *P. densiflora* in the early germination stage were mounted on a glass slide for  
150 stereomicroscopy and light microscopy. Components of RETs were mounted in sterile water or  
151 following staining on a glass slide for bright-field and fluorescence microscopy using a light  
152 microscope (Olympus BX50; Olympus, Tokyo, Japan). All staining and observation processes  
153 were conducted on at least three technical replicates.

154 To visualize the viability of AC-DCs shed from the root cap, live and dead cells were stained  
155 with fluorescein diacetate solution ( $1 \mu\text{g}\cdot\text{mL}^{-1}$  in phosphate-buffered saline [PBS]) and 0.01%  
156 (v/v) Evans blue solution, respectively. Cells were stained and observed within 15 min of  
157 separation from the root. The same process was also performed on the separated samples  
158 incubated in a 1.5 mL tube containing 200  $\mu\text{L}$  sterile water at 25°C for 2, 4, 7, 14, and 28 days.  
159 Five replicates were prepared for each timepoint.

160 AC-DCs were stained using 1% or 3% (v/v) crystal violet (CV) solution, and the mucilage  
161 layer was visualized using CV of the same concentration and 0.4% (v/v) India ink solution;  
162 sterile water was used as the solvent for both solutions.

163 The CV solution and calcofluor white M2R solution ( $1 \text{ mg}\cdot\text{mL}^{-1}$  in sterile water) were used to  
164 clarify the origin of branched strands frequently found as AC-DCs shed. Moreover, actin  
165 filaments in AC-DCs were visualized under the following conditions, at room temperature: cells  
166 were fixed with 4% (v/v) paraformaldehyde in PBS (pH 7.0) for 15 min, rinsed with PBS for 30  
167 s, incubated in 0.1% (v/v) Triton X-100 solution in PBS for 15 min, rinsed with PBS for 30 s  
168 twice, stained with 0.1  $\mu\text{M}$  Acti-stain 555 fluorescent phalloidin (Cytoskeleton Inc., Denver, CO,  
169 USA) for 30 min, rinsed with PBS for 30 s three times, stained with 4',6-diamidino-2-  
170 phenylindole (DAPI) as a counterstain for 30 s, and rinsed with PBS for 30 s.

171 ExDNA released from AC-DCs was labeled using 1  $\mu\text{M}$  SYTOX Green (Thermo Fisher  
172 Scientific, Waltham, MA, USA). Stock solutions were made following the manufacturer's  
173 instructions.

174

### 175 **Visualization of rhizobacteria trapped by RETs**

176 For the observations, four bacterial strains, mainly *Bacillus* sp. strain O-EM7 (BC O-EM7)  
177 and *Paraburkholderia* sp. strain O-NM9 (PS O-NM9) were pre-cultivated on YG agar medium  
178 at 25°C for 2 days, and then were suspended in sterile water and adjusted to an optical density at  
179 600 nm (OD<sub>600</sub>) of 0.05. Next, the tip of a primary root was immersed in a 1.5 mL tube  
180 containing 200 µL suspension and was incubated in darkness at 25°C for 8 h or 2 days. After  
181 incubation, RETs were detached from the root cap using tweezers, rinsed with sterile water  
182 twice, then stained with 3% CV solution and 1 µM SYTOX Green.

183

### 184 **Colony-forming unit assay**

185 We performed a colony-forming unit (CFU) assay to confirm the effects of the presence or  
186 absence of RETs on bacterial colonization in the early stage of *P. densiflora* rhizosphere  
187 development. Root tips, processed via swelling treatment, were immersed in bacterial  
188 suspensions (OD<sub>600</sub> = 0.05), and RETs were removed under aseptic conditions before and 2 days  
189 after incubation at 25°C, respectively. Root tips without RETs removed were used as the control  
190 (n = 5). Incubated samples were separated from the seed, leaving a root tip of 5 mm, gently  
191 rinsed with sterile water twice, homogenized using a micropestle, and suspended in 1 mL sterile  
192 water. The suspensions were used as a stock solution, serially diluted up to 100,000 times, and  
193 100 µL each dilution was spread on two dishes of YG agar medium per dilution step. After  
194 incubation at 25°C for 2 days, bacterial colonies formed on the medium were counted; the  
195 average number of colonies in two dishes that fell within 30–300 was adopted, and the values  
196 were log-transformed (Log<sub>10</sub> CFU) for statistical analysis.

197

### 198 **Detection of total ROS in response to contact with rhizobacteria**

199 To evaluate the defense response of the RETs induced by contact with rhizobacteria, we  
200 examined ROS production, which is an early defense signal in plant root immunity (Boller and  
201 Felix 2009). After swelling treatment, RETs were stripped from the root tip, immersed in 200  $\mu$ L  
202 each bacterial suspension ( $OD_{600} = 0.05$ ), and incubated in darkness at 25°C for 4 h. In addition,  
203 RETs were treated with 1  $\mu$ M flg22 (Alpha Diagnostic International Inc., San Antonio, TX,  
204 USA), a representative MAMP peptide derived from bacterial flagella (Millet et al. 2010). Sterile  
205 water was used as the control, and five replicates of each treatment were performed. After  
206 rinsing twice with Hank's balanced salt solution without phenol red (HBSS-), RETs were stained  
207 using the fluorescent probe ROS Assay Kit -Highly Sensitive DCFH-DA- (Dojindo Laboratories,  
208 Kumamoto, Japan) at 25°C for 30 min. The working solution was prepared following the  
209 manufacturer's instructions. Stained samples were rinsed twice with HBSS-, and then five  
210 random locations per sample were imaged under fluorescence microscopy within 2 h of staining  
211 using the following conditions (except when images were captured at 1000 $\times$  magnification):  
212 2040  $\times$  1536 pixels; 200 $\times$  magnification; ISO200; 12 ms exposure; RGB values of 0.7:1.0:2.1; 8  
213 bits; and tiff. extension. Total ROS production, here considered to indicate the degree of cellular  
214 sensitivity to the treatments, was calculated as the relative fluorescence intensity per sample,  
215 using Fiji (ImageJ ver. 1.53q) software (Schindelin et al. 2012). First, the original image was  
216 divided into three colors (red, blue, and green), and red was subtracted from green. Then, an  
217 image was generated using the Li model and a range of 25–255 as the threshold value. Finally,  
218 the number of pixels corresponding to the threshold was counted.

219

## 220 **Image processing**

221 Fiji, Inkscape ver. 1.0 (<https://inkscape.org/>), and GIMP ver. 2.10.20 (<https://www.gimp.org/>)  
222 software were used to export and process each figure. Except for those used for the image  
223 analyses, when processing images after capturing, the entire image was altered and only

224 brightness and contrast were modulated. Movies (Online Resources 1–8) were processed using  
225 DaVinci Resolve ver. 18.1.2 (<https://www.blackmagicdesign.com/products/davinciresolve/>)  
226 under the same conditions.

227

## 228 **Statistical analysis**

229 The significance of differences among treatments in the CFU and ROS detection assays were  
230 analyzed by one-way analysis of variance using the Tukey's HSD test. Data processing and  
231 analysis, and graph plotting were performed using R ver. 4.0.4 (R Core Team 2021).

232

## 233 **Results**

### 234 **Visualization of RETs in the primary root of *P. densiflora***

235 Figure 1 presents an overview of the RETs and their major components in the primary root of  
236 *P. densiflora*. RBC shedding, RBLC detachment, and root mucilage percolation from the root  
237 cap were immediately observed when root tips that had not yet undergone swelling treatment  
238 were immersed in the solutions (Fig. 1c, e, and f; Online Resources 1 and 2). The root cap  
239 released mainly elliptic and oblong RBCs from the apex, and sheath-shaped and long layers of  
240 RBLCs from the lateral sides. CV readily stained each component, revealing their dispersal to  
241 cover the root tip; membranous mucilage was visualized particularly well (Fig. 1f, Fig. 2). Most  
242 of the AC-DCs remained viable in sterile water immediately after isolation from the root cap  
243 (Fig. 1d). We confirmed vigorous cytoplasmic streaming initially and even after 7 days of  
244 isolation (Online Resources 3–5); some cells remained viable until day 28 (Fig. S1). However,  
245 cells mounted without liquid wilted and died quickly. Branched strands were observed to  
246 protrude from both living and dead cells, particularly at the joints between RBLCs and at the  
247 longitudinal tip of the RBCs (Fig. 1g–i). Damaged AC-DCs experiencing plasmolysis tended to  
248 discharge copious amounts of strands compared to live cells (Fig. 1g). They were readily stained

249 with CV and CW, and slightly stained with Acti-stain 555 phalloidin; however, no labeling was  
250 observed after application of two fluorescent dyes for DNA, DAPI and SYTOX Green (Fig. 1g–  
251 l). Actin filaments in the AC-DCs had structures similar to the strands, but we could not confirm  
252 whether they were identical (Fig. 1j). SYTOX Green stained exDNA, which visualized their  
253 spread in thread-like or web-like structures (Fig. 1m–o, Fig. 3); these structures were observed  
254 during unraveling of the spherical structure of the cell nucleus (Fig. 3a, b), and some structures  
255 spread more than five times the area of a single RBC (Fig. 3c). The unfolding of exDNA was  
256 found both with or without microorganisms, and we could not confirm active secretion during  
257 our observations.

258

### 259 **Trapping of rhizobacteria by RETs**

260 We demonstrated that rhizobacterial cells were trapped by root mucilage and exDNA using  
261 CV and SYTOX Green, respectively (Fig. 2, Fig. 3). Bacterial cells, which exhibited active  
262 swarming in suspension, showed minimal movement after adhering to the mucilage, and were  
263 not liberated when the solution was gently agitated (Fig. 2c, e, and f; Online Resources 6–8).  
264 Branched strands, similar to frameworks, were also frequently entangled in the mucilage layer  
265 with bacterial cells (Fig. 2d). SYTOX Green is a DNA-specific dye that cannot penetrate living  
266 cell membranes (Wen et al. 2017); hence, only dead cells, including bacteria, show a  
267 fluorescence response. SYTOX Green staining visualized some dead bacterial cells trapped by  
268 exDNA that had spread in thread-like or web-like structures within the RETs (Fig. 3c, d, and e).  
269 However, bacteria trapped by exDNA were localized compared to those in the mucilage layer,  
270 and many living bacterial cells attached to the mucilage were observed under bright-field  
271 conditions (Fig. 3f).

272 The CFU assay results indicated that RETs could contribute to bacterial colonization in the  
273 early germination stage of the rhizosphere of *P. densiflora*. By contrast, RET removal (Fig. 4a)

274 tended to reduce CFU counts, particularly those removed after incubation, which significantly  
275 impaired the CFU counts of all bacterial strains (Fig. 4b). There were no differences in the  
276 morphological features of bacterial colonies formed on the medium among these treatments.

277

### 278 **Production of ROS in response to rhizobacteria**

279 Fluorescent staining for total ROS revealed the production of ROS in AC-DCs (Fig. 5). An  
280 early fluorescence response to bacterial MAMP perception, the oxidative burst (Boller and Felix  
281 2009; Zipfel 2009), could be roughly divided into two patterns based on the fluorescence signal:  
282 in the first pattern, fluorescence was isolated to cellular organelles; in the second pattern,  
283 fluorescence was observed in the whole cell, except the nucleus (Fig. 5b). A comparison of the  
284 relative fluorescence intensity based on image analysis revealed that co-incubation with  
285 rhizobacterial strains tended to enhance the total ROS production of AC-DCs (Fig. 5c). Two  
286 *Paraburkholderia* strains, PM O-EM8 and PF T-NM22, significantly differed from the control  
287 treatment, and the latter had the highest values. However, BC O-EM7 and PS O-NM9 did not  
288 result in significant differences in the fluorescence response compared to the control group;  
289 fluorescence responses were also detected in a wide range of intracellular organelles such as  
290 plastids, mitochondria, and peroxisomes, similar PM O-EM8 and PF T-NM22 (Fig. 5a, c). In  
291 addition, the ROS levels detected after flg22 treatment did not significantly differ from the  
292 control, and were lower than those after co-incubation with the bacterial suspensions.

293

### 294 **Discussion**

295 The number of AC-DCs produced and the pattern they form vary among plant species. For  
296 instance, the root cap of *P. sativum* produces many RBCs, whereas *A. thaliana* mainly releases  
297 cells connected in layers (Hawes et al. 1998; Vicié et al. 2005; Driouich et al. 2019). Hamamoto  
298 et al. (2006) demonstrated that these differences among dicotyledonous angiosperms are

299 attributable to variation in RAM organization structures. Meanwhile, Carreras et al. (2020)  
300 observed that two Fabaceae tree species, *A. raddiana* and *T. indica*, have open RAMs, similar to  
301 *P. sativum*, and yet release mainly sheaths of RBLCs. Our observations of the woody  
302 gymnosperm *P. densiflora* matched neither *A. thaliana* nor *P. sativum* but were relatively similar  
303 to *A. raddiana* among the species studied to date. Therefore, our results partly corroborate those  
304 of Hamamoto et al. (2006) in that *P. densiflora* has a different RAM structure than *A. thaliana*  
305 and *P. sativum* (Imaichi et al. 2018). These findings suggest that additional factors, such as  
306 differences between angiosperms and gymnosperms, differences between dicots and monocots,  
307 and the types of symbioses with microorganisms, should be considered in addition to RAM  
308 structure. Furthermore, the pectin-degrading enzymes pectin methylesterase and  
309 polygalacturonase are reportedly involved in such cell separation (Hawes and Lin 1990; Wen et  
310 al. 1999; Driouich et al. 2007). In *A. thaliana*, Kamiya et al. (2016) showed that three NAC  
311 transcription factors, *SOMBRERO*, *BEARSKIN (BRN) 1*, and *BRN2*, regulate the expression of  
312 *ROOT CAP POLYGALACTURONASE (RCPG)* in polygalacturonase secretion; of these, at least  
313 *BRN1* directly binds to *RCPG* promoter. Karve et al. (2016) also revealed that the transcription  
314 factor NIN-LIKE PROTEIN 7 controls the cell wall-loosening enzyme CELLULASE 5, thereby  
315 enabling the release of RBLCs in *A. thaliana*. Comparing the expression dynamics of target  
316 genes among plant species may help categorize their cell detachment patterns.

317 In *Pinus* species, the viability and long-term survival of AC-DCs still require examination,  
318 although such cells have been assessed immediately after detachment (Hawse and Pueppke  
319 1986). Our tests, performed under non-nutritional liquid conditions, support the previous study,  
320 which used *Glycine max* and *P. sativum* (until 31 days), suggest that the AC-DCs of *P.*  
321 *densiflora* could survive for more extended periods under favorable conditions. In addition,  
322 given that RET components are produced from living AC-DCs (Driouich et al. 2019), these  
323 findings indicate that soil nutrient deficiencies or drought stress cause dysfunction of RETs

324 under field conditions and may lead to the death of young seedlings.

325 We confirmed that the strand structures were not stained with either of two DNA-specific  
326 fluorescent probes. A recent study described entangled strands readily stained with CV as  
327 “barbed wire” (Wen et al. 2017, p. 974) structures, and they could be digested by DNase I or II  
328 (Wen et al. 2017; Huskey et al. 2019). Moreover, Ropitiaux et al. (2019) reported that cellulose  
329 and xyloglucan present as a dense fibrous network in the root mucilage and maintain AC-DC  
330 attachments. These findings are reasonably consistent with our histochemical observations using  
331 CW (staining  $\beta$ -linked polysaccharides) and phalloidin (staining F-actin), indicating that the  
332 strands observed in this study differ from exDNA, and their origin is the cell wall or  
333 cytoskeleton. Although the role of branched strands in RETs remains unclear, we postulate that  
334 they strengthen the structure of mucilage and function as a physical scaffold that binds bacteria,  
335 which are found frequently in the mucilage layer. This hypothesis does not conflict with the facts  
336 that RBCs can show selectivity for bacteria (Hawes and Pueppke 1989) and root mucilage is a  
337 carbon source for rhizobacteria, influencing their community compositions (Knee et al. 2001;  
338 Benizri et al. 2007). Thus, these strands may be considered a nonlethal and mucilage-coated  
339 component for rhizobacterial trapping, which implies that AC-DCs have some functions even  
340 after cell death.

341 Based on our observations, bacterial cells did not survive trapping by exDNA. Defensin  
342 peptides and exDNA have bactericidal functions in RETs. In exDNA, histone H4 (the only  
343 DNA-binding protein found in plants) induces microorganism death by disrupting their cell  
344 membranes (Wen et al. 2007; Hawes et al. 2012; Driouich et al. 2019; Monticolo et al. 2020).  
345 Thus, exDNA from AC-DCs in *P. densiflora* likely has a lethal effect against bacteria, whereas  
346 while root mucilage enables nonlethal trapping. Our CFU assay-based results supported these  
347 observations; consequently, the RETs of *P. densiflora* should facilitate commensal and beneficial  
348 bacterial colonization in the rhizosphere despite being capable of killing bacteria. However,

349 additional studies will be needed to fully elucidate the effects of exDNA against rhizobacteria;  
350 for instance, they may have a controlling effect to prevent bacterial overgrowth in the  
351 rhizosphere. Future studies also should focus on the immune-evasive and -suppressive  
352 capabilities of bacteria, i.e., degrading exDNA, hiding MAMPs, and modulating hormonal  
353 signaling pathways (Tran et al. 2016; Yu et al. 2019; Teixeira et al. 2021).

354 The four rhizobacterial strains induced ROS production from the host tree AC-DCs of the *P.*  
355 *densiflora*. A recent study on *A. thaliana* elucidated a feedback loop, that is, an interaction  
356 between host plant root and beneficial bacteria; the study showed that bacterial colonization  
357 elicited a root immune response and ROS production, followed by auxin stimulation, thereby  
358 promoting bacterial survival in the rhizosphere (Tzipilevich et al. 2021). Our results may be  
359 relevant to this cycle in that the bacterial strains were not excluded from the rhizosphere.  
360 Moreover, we assessed three *Paraburkholderia* strains, of which PF T-NM22 induced a notably  
361 high level of ROS production. The four bacterial strains investigated in this study belong to two  
362 genera, *Bacillus* and *Paraburkholderia*. Both genera are common beneficial rhizobacteria  
363 (Santoyo et al. 2016), and the latter prime plant immune responses, functioning as a first line of  
364 defense against pathogens (Carrión et al. 2018; Tringe 2019; Leitão et al. 2021; del Carmen  
365 Orozco-Mosqueda et al. 2022). Therefore, our results show the indirect contribution of  
366 rhizobacteria to host root defense and indicate that root-associated bacteria could be a component  
367 of RETs, which is equivalent to “an additional layer of the plant immune system” (Teixeira et al.  
368 2019, p. 13).

369 The present findings reveal that RETs function in the early growth stage of *P. densiflora*. To  
370 the best of our knowledge, this is the first study to investigate RETs in an ECM woody  
371 gymnosperm and their influence on rhizobacterial colonization. However, our findings are  
372 limited to only the primary roots, given that root morphology changes anatomically during  
373 growth and turnover (Brunner and Scheidegger 1992; McCrady and Comerford 1998; Peterson et

374 al. 1999), and the mechanisms of metabolites vary among root zones within an individual root  
375 (Sasse et al. 2018). Thus, it would be beneficial to investigate whether RETs function in mature  
376 lateral root systems.

377

### 378 **Author Contribution Statement**

379 MS conceived the research plans and experimental designs; NM and KF supervised and  
380 improved them. MS performed the experiments, microscopic observations, and data analyses and  
381 drafted the manuscript; NM and KF critically reviewed and provided feedback. All authors  
382 contributed to the revision of the manuscript and approved the final version for submission.

383

### 384 **Acknowledgments**

385 This work was supported by Japan Society for the Promotion of Science KAKENHI grant  
386 number JP21J12127.

387

### 388 **Declarations**

### 389 **Conflict of interest**

390 The authors have no conflicts of interest associated with the article.

391

### 392 **References**

393 Atkinson N J, Urwin P E (2012) The interaction of plant biotic and abiotic stresses: from genes  
394 to the field. *J Exp Bot* 63:3523–3543. <https://doi.org/10.1093/jxb/ers100>

395 Badri D V, Vivanco J M (2009) Regulation and function of root exudates. *Plant Cell Environ*  
396 32:666–681. <https://doi.org/10.1111/j.1365-3040.2009.01926.x>

397 Benizri E, Nguyen C, Piutti S, Slezack-Deschaumes S, Philippot L (2007) Additions of maize  
398 root mucilage to soil changed the structure of the bacterial community. *Soil Biol Biochem*

399 39:1230–1233. <https://doi.org/10.1016/j.soilbio.2006.12.026>

400 Boller T, Felix G (2009) A renaissance of elicitors: perception of microbe-associated molecular  
401 patterns and danger signals by pattern-recognition receptors. *Annu Rev Plant Biol* 60:379–  
402 406. <https://doi.org/10.1146/annurev.arplant.57.032905.105346>

403 Brinkmann V, Reichard U, Goosmann C, Fauler B, Uhlemann Y, Weiss D S, Weinrauch Y,  
404 Zychlinsky A (2004) Neutrophil extracellular traps kill bacteria. *Science* 303:1532–1535.  
405 <https://doi.org/10.1126/science.1092385>

406 Brunner I, Scheidegger C (1992) Ontogeny of synthesized *Picea abies* (L.) Karst.–*Hebeloma*  
407 *crustuliniforme* (Bull. ex St Amans) Qué. ectomycorrhizas. *New Phytol* 120:359–369.  
408 <https://doi.org/10.1111/j.1469-8137.1992.tb01076.x>

409 Carreras A, Bernard S, Durambur G, Gügi B, Loutelier C, Pawlak B, Boulogne I, Viché M,  
410 Driouich A, Goffner D, Follet-Gueye M-L (2020) In vitro characterization of root  
411 extracellular trap and exudates of three Sahelian woody plant species. *Planta* 251:1–18.  
412 <https://doi.org/10.1007/s00425-019-03302-3>

413 Carrión V J, Cordovez V, Tyc O, Etalo D W, de Bruijn I, de Jager V C, Medema M H, Eberl L,  
414 Raaijmakers J M (2018) Involvement of Burkholderiaceae and sulfurous volatiles in  
415 disease-suppressive soils. *The ISME J* 12:2307–2321. [https://doi.org/10.1038/s41396-018-](https://doi.org/10.1038/s41396-018-0186-x)  
416 0186-x

417 Cook D E, Mesarich C H, Thomma B P (2015) Understanding plant immunity as a surveillance  
418 system to detect invasion. *Annu Rev Phytopathol* 53:541–563.  
419 <https://doi.org/10.1146/annurev-phyto-080614-120114>

420 Cramer G R, Urano K, Delrot S, Pezzotti M, Shinozaki K (2011) Effects of abiotic stress on  
421 plants: a systems biology perspective. *BMC Plant Biol* 11:1–14.  
422 <https://doi.org/10.1186/1471-2229-11-163>

423 del Carmen Orozco-Mosqueda M, Fadiji A E, Babalola O O, Glick B R, Santoyo G (2022)

424 Rhizobiome engineering: Unveiling complex rhizosphere interactions to enhance plant  
425 growth and health. *Microbiol Res* 263:127137.  
426 <https://doi.org/10.1016/j.micres.2022.127137>

427 De Vleeschauwer D, Höfte M (2009) Rhizobacteria-induced systemic resistance. *Adv Bot Res*  
428 51:223–281. [https://doi.org/10.1016/S0065-2296\(09\)51006-3](https://doi.org/10.1016/S0065-2296(09)51006-3)

429 Driouich A, Durand C, Vicié-Gibouin M (2007) Formation and separation of root border cells.  
430 *Trends Plant Sci* 12:14–19. <https://doi.org/10.1016/j.tplants.2006.11.003>

431 Driouich A, Follet-Gueye M-L, Vicié-Gibouin M, Hawes M (2013) Root border cells and  
432 secretions as critical elements in plant host defense. *Curr Opin Plant Biol* 16:489–495.  
433 <https://doi.org/10.1016/j.pbi.2013.06.010>

434 Driouich A, Gaudry A, Pawlak B, Moore J P (2021) Root cap–derived cells and mucilage: a  
435 protective network at the root tip. *Protoplasma* 258: 1179–1185.  
436 <https://doi.org/10.1007/s00709-021-01660-y>

437 Driouich A, Smith C, Ropitiaux M, Chambard M, Boulogne I, Bernard S, Follet-Gueye M-L,  
438 Vicié M, Moore J (2019) Root extracellular traps *versus* neutrophil extracellular traps in  
439 host defence, a case of functional convergence? *Biol Rev* 94:1685–1700.  
440 <https://doi.org/10.1111/brv.12522>

441 Endo I, Tange T, Osawa H (2011) A cell-type-specific defect in border cell formation in the  
442 *Acacia mangium* root cap developing an extraordinary sheath of sloughed-off cells. *Ann*  
443 *Bot* 108:279–290. <https://doi.org/10.1093/aob/mcr139>

444 Fortier M, Lemaitre V, Gaudry A, Pawlak B, Driouich A, Follet-Gueye M-L, Vicié M (2023) A  
445 fine-tuned defense at the pea root caps: Involvement of border cells and arabinogalactan  
446 proteins against soilborne diseases. *Front Plant Sci* 14:1132132.  
447 <https://doi.org/10.3389/fpls.2023.1132132>

448 Ganesh A, Shukla V, Mohapatra A, George A P, Bhukya D P N, Das K K, Kola V S R, Suresh

449 A, Ramireddy E (2022) Root cap to soil interface: a driving force toward plant adaptation  
450 and development. *Plant Cell Physiol* 63:1038–1051. <https://doi.org/10.1093/pcp/pcac078>

451 Gonthier P, Nicolotti G (Eds.) (2013) *Infectious forest diseases*. Cabi, UK

452 Hamamoto L, Hawes M C, Rost T L (2006) The production and release of living root cap border  
453 cells is a function of root apical meristem type in dicotyledonous angiosperm plants. *Ann*  
454 *Bot* 97:917–923. <https://doi.org/10.1093/aob/mcj602>

455 Hawes M, Allen C, Turgeon B G, Curlango-Rivera G, Minh Tran T, Huskey D A, Xiong Z  
456 (2016) Root border cells and their role in plant defense. *Annu Rev Phytopathol* 54:143–161.  
457 <https://doi.org/10.1146/annurev-phyto-080615-100140>

458 Hawes M C, Bengough G, Cassab G, Ponce G (2003) Root caps and rhizosphere. *J Plant Growth*  
459 *Regul* 21:352–367. <https://doi.org/10.1007/s00344-002-0035-y>

460 Hawes M C, Brigham L A, Wen F, Woo H H, Zhu Y (1998) Function of root border cells in  
461 plant health: Pioneers in the rhizosphere. *Annu Rev Phytopathol* 36:311–327.  
462 <https://doi.org/10.1146/annurev.phyto.36.1.311>

463 Hawes M C, Curlango-Rivera G, Xiong Z, Kessler J O (2012) Roles of root border cells in plant  
464 defense and regulation of rhizosphere microbial populations by extracellular DNA  
465 ‘trapping.’ *Plant and Soil* 355:1–16. <https://doi.org/10.1007/s11104-012-1218-3>

466 Hawes M C, Lin H J (1990) Correlation of pectolytic enzyme activity with the programmed  
467 release of cells from root caps of pea (*Pisum sativum*). *Plant Physiol* 94:1855–1859.  
468 <https://doi.org/10.1104/pp.94.4.1855>

469 Hawes M C, Pueppke S G (1986) Sloughed peripheral root cap cells: yield from different species  
470 and callus formation from single cells. *Am J Bot* 73:1466–1473.  
471 <https://doi.org/10.1002/j.1537-2197.1986.tb10892.x>

472 Hawes M C, Pueppke S G (1989) Variation in binding and virulence of *Agrobacterium*  
473 *tumefaciens* chromosomal virulence (*chv*) mutant bacteria on different plant species. *Plant*

474       Physiol 91:113–118. <https://doi.org/10.1104/pp.91.1.113>

475   Huot B, Yao J, Montgomery B L, He S Y (2014) Growth–defense tradeoffs in plants: a  
476       balancing act to optimize fitness. *Mol plant* 7:1267–1287.  
477       <https://doi.org/10.1093/mp/ssu049>

478   Huskey D A, Curlango-Rivera G, Hawes M C (2019) Use of rhodizonic acid for rapid detection  
479       of root border cell trapping of lead and reversal of trapping with DNase. *Appl Plant Sci*  
480       7:e01240. <https://doi.org/10.1002/aps3.1240>

481   Imaichi R, Moritoki N, Solvang H K (2018) Evolution of root apical meristem structures in  
482       vascular plants: plasmodesmatal networks. *Am J Bot* 105:1453–1468.  
483       <https://doi.org/10.1002/ajb2.1153>

484   Kamiya M, Higashio S Y, Isomoto A, Kim J M, Seki M, Miyashima S, Nakajima K (2016)  
485       Control of root cap maturation and cell detachment by BEARSKIN transcription factors in  
486       *Arabidopsis*. *Development* 143:4063–4072. <https://doi.org/10.1242/dev.142331>

487   Karve R, Suárez-Román F, Iyer-Pascuzzi A S (2016) The transcription factor NIN-LIKE  
488       PROTEIN7 controls border-like cell release. *Plant Physiol* 171:2101–2111.  
489       <https://doi.org/10.1104/pp.16.00453>

490   Knee E M, Gong F C, Gao M, Teplitski M, Jones A R, Foxworthy A, Mort A J, Bauer W D  
491       (2001) Root mucilage from pea and its utilization by rhizosphere bacteria as a sole carbon  
492       source. *Mol Plant-Microbe Interact* 14:775–784.  
493       <https://doi.org/10.1094/MPMI.2001.14.6.775>

494   Kuzyakov Y, Razavi B S (2019) Rhizosphere size and shape: temporal dynamics and spatial  
495       stationarity. *Soil Biol Biochem* 135:343–360. <https://doi.org/10.1016/j.soilbio.2019.05.011>

496   Leitão F, Pinto G, Amaral J, Monteiro P, Henriques I (2022) New insights into the role of  
497       constitutive bacterial rhizobiome and phenolic compounds in two *Pinus* spp. with  
498       contrasting susceptibility to pine pitch canker. *Tree Physiol* 42:600–615.

499 <https://doi.org/10.1093/treephys/tpab119>

500 Liu Q, Li K, Guo X, Ma L, Guo Y, Liu Z (2019) Developmental characteristics of grapevine  
501 seedlings root border cells and their response to  $\rho$ -hydroxybenzoic acid. *Plant and Soil*  
502 443:199–218. <https://doi.org/10.1007/s11104-019-04220-9>

503 Martín-Pinto P, Pajares J, Díez J (2006) In vitro effects of four ectomycorrhizal fungi, *Boletus*  
504 *edulis*, *Rhizopogon roseolus*, *Laccaria laccata* and *Lactarius deliciosus* on *Fusarium*  
505 damping off in *Pinus nigra* seedlings. *New For* 32:323–334.  
506 <https://doi.org/10.1007/s11056-006-9006-7>

507 McCrady R L, Comerford N B (1998) Morphological and anatomical relationships of loblolly  
508 pine fine roots. *Trees* 12:431–437. <https://doi.org/10.1007/s004680050171>

509 Millet Y A, Danna C H, Clay N K, Songnuan W, Simon M D, Werck-Reichhart D, Ausubel F M  
510 (2010) Innate immune responses activated in Arabidopsis roots by microbe-associated  
511 molecular patterns. *The Plant Cell* 22:973–990. <https://doi.org/10.1105/tpc.109.069658>

512 Mohanram S, Kumar P (2019) Rhizosphere microbiome: revisiting the synergy of plant-microbe  
513 interactions. *Ann Microbiol* 69:307–320. <https://doi.org/10.1007/s13213-019-01448-9>

514 Monticolo F, Palomba E, Termolino P, Chiaiese P, De Alteriis E, Mazzoleni S, Chiusano M L  
515 (2020) The role of DNA in the extracellular environment: a focus on NETs, RETs and  
516 biofilms. *Front Plant Sci* 11:589837. <https://doi.org/10.3389/fpls.2020.589837>

517 Motte H, Vanneste S, Beeckman T (2019) Molecular and environmental regulation of root  
518 development. *Annu Rev Plant Biol* 70:465–488. <https://doi.org/10.1146/annurev-arplant-050718-100423>

520 Peterson C A, Enstone D E, Taylor J H (1999) Pine root structure and its potential significance  
521 for root function. *Plant and Soil* 217:205–213. <https://doi.org/10.1023/A:1004668522795>

522 Plancot B, Santaella C, Jaber R, Kiefer-Meyer M C, Follet-Gueye M-L, Leprince J, Gattin I,  
523 Souc C, Driouich A, Vicré-Gibouin M (2013) Deciphering the responses of root border-like

524 cells of Arabidopsis and flax to pathogen-derived elicitors. *Plant Physiol* 163:1584–1597.  
525 <https://doi.org/10.1104/pp.113.222356>

526 Policelli N, Bruns T D, Vilgalys R, Nuñez M A (2019) Suilloid fungi as global drivers of pine  
527 invasions. *New Phytol* 222:714–725. <https://doi.org/10.1111/nph.15660>

528 R Core Team (2021). R: A language and environment for statistical computing. R Foundation for  
529 Statistical Computing, Vienna, Austria. URL <https://www.R-project.org/>.

530 Ropitiaux M, Bernard S, Follet-Gueye M L, Vicré M, Boulogne I, Driouich A (2019) Xyloglucan  
531 and cellulose form molecular cross-bridges connecting root border cells in pea (*Pisum*  
532 *sativum*). *Plant Physiol Biochem* 139:191–196.  
533 <https://doi.org/10.1016/j.plaphy.2019.03.023>

534 Santoyo G, Moreno-Hagelsieb G, del Carmen Orozco-Mosqueda M, Glick B R (2016) Plant  
535 growth-promoting bacterial endophytes. *Microbiol Res* 183:92–99.  
536 <https://doi.org/10.1016/j.micres.2015.11.008>

537 Sasse J, Martinoia E, Northen T (2018) Feed your friends: do plant exudates shape the root  
538 microbiome? *Trends Plant Sci* 23:25–41. <https://doi.org/10.1016/j.tplants.2017.09.003>

539 Schindelin J, Arganda-Carreras I, Frise E et al (2012) Fiji: an open-source platform for  
540 biological-image analysis. *Nat Methods* 9:676–682. <https://doi.org/10.1038/nmeth.2019>

541 Suzuki N, Rivero R M, Shulaev V, Blumwald E, Mittler R (2014) Abiotic and biotic stress  
542 combinations. *New Phytol* 203:32–43. <https://doi.org/10.1111/nph.12797>

543 Teixeira P J, Colaianni N R, Law T F, Conway J M, Gilbert S, Li H, Salas-González I, Panda D,  
544 Del Risco N M, Finkel O M, Castrillo G, Mieczkowski P, Jones C D, Dangl J L (2021)  
545 Specific modulation of the root immune system by a community of commensal bacteria.  
546 *PNAS* 118:e2100678118. <https://doi.org/10.1073/pnas.2100678118>

547 Teixeira P J P, Colaianni N R, Fitzpatrick C R, Dangl J L (2019). Beyond pathogens: microbiota  
548 interactions with the plant immune system. *Curr Opin Microbiol* 49:7–17.

549 <https://doi.org/10.1016/j.mib.2019.08.003>

550 Tran T M, MacIntyre A, Hawes M, Allen C (2016) Escaping underground nets: extracellular  
551 DNases degrade plant extracellular traps and contribute to virulence of the plant pathogenic  
552 bacterium *Ralstonia solanacearum*. PLoS Pathog 12:e1005686.  
553 <https://doi.org/10.1371/journal.ppat.1005686>

554 Tringe S G (2019) A layered defense against plant pathogens. Science 366:568–569.  
555 <https://doi.org/10.1126/science.aaz5619>

556 Tzipilevich E, Russ D, Dangl J L, Benfey P N (2021) Plant immune system activation is  
557 necessary for efficient root colonization by auxin-secreting beneficial bacteria. Cell Host  
558 Microbe 29:1507–1520. <https://doi.org/10.1016/j.chom.2021.09.005>

559 Vicré M, Santaella C, Blanchet S, Gateau A, Driouich A (2005) Root border-like cells of  
560 Arabidopsis. Microscopical characterization and role in the interaction with rhizobacteria.  
561 Plant Physiol 138:998–1008. <https://doi.org/10.1104/pp.104.051813>

562 Weisburg W G, Barns S M, Pelletier D A, Lane D J (1991) 16S ribosomal DNA amplification  
563 for phylogenetic study. J Bacteriol 173:697–703. [https://doi.org/10.1128/jb.173.2.697-](https://doi.org/10.1128/jb.173.2.697-703.1991)  
564 [703.1991](https://doi.org/10.1128/jb.173.2.697-703.1991)

565 Wen F, Curlango-Rivera G, Huskey D A, Xiong Z, Hawes M C (2017) Visualization of  
566 extracellular DNA released during border cell separation from the root cap. Am J Bot  
567 104:970–978. <https://doi.org/10.3732/ajb.1700142>

568 Wen F, VanEtten H D, Tsapralis G, Hawes M C (2007) Extracellular proteins in pea root tip and  
569 border cell exudates. Plant Physiol 143:773–783. <https://doi.org/10.1104/pp.106.091637>

570 Wen F, White G J, VanEtten H D, Xiong Z, Hawes M C (2009) Extracellular DNA is required  
571 for root tip resistance to fungal infection. Plant Physiol 151:820–829.  
572 <https://doi.org/10.1104/pp.109.142067>

573 Wen F, Zhu Y, Hawes M C (1999) Effect of pectin methylesterase gene expression on pea root

574 development. *The Plant Cell* 11:1129–1140. <https://doi.org/10.1105/tpc.11.6.1129>

575 Yu K, Pieterse C M, Bakker P A, Berendsen R L (2019) Beneficial microbes going underground  
576 of root immunity. *Plant Cell Environ* 42:2860–2870. <https://doi.org/10.1111/pce.13632>

577 Zhang H, Yu H, Tang M (2017) Prior contact of *Pinus tabulaeformis* with ectomycorrhizal fungi  
578 increases plant growth and survival from damping-off. *New For* 48 855–866.  
579 <https://doi.org/10.1007/s11056-017-9601-9>

580 Zipfel C (2009) Early molecular events in PAMP-triggered immunity. *Curr Opin Plant Biol*  
581 12:414–420. <https://doi.org/10.1016/j.pbi.2009.06.003>

582

583

584

585

586

587

588

589

590

591

592

593

594

595

596

597

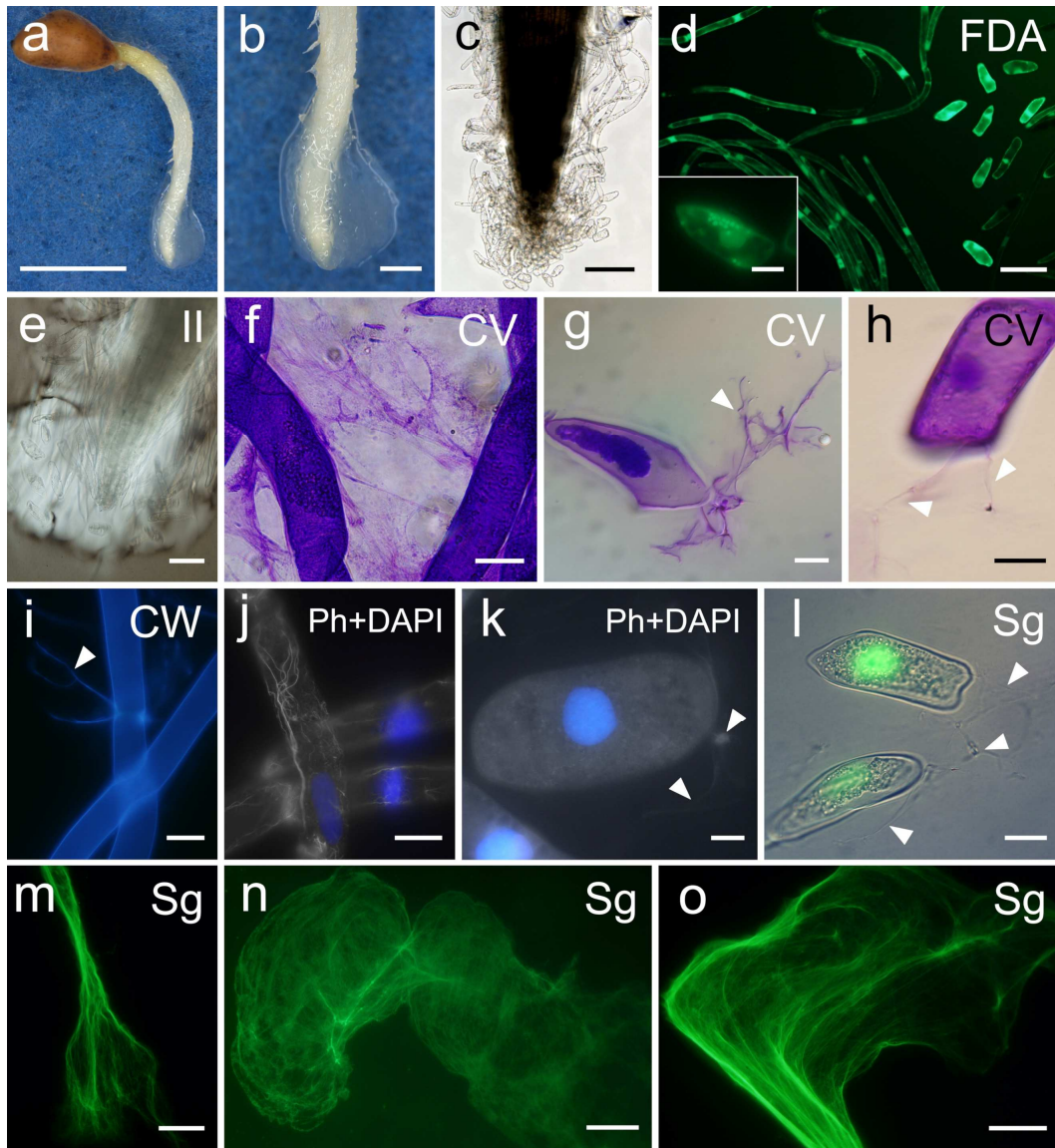
598  
599  
600  
601  
602  
603  
604  
605  
606  
607  
608  
609  
610  
611

**Table 1** Root-associated bacterial strains isolated from the rhizosphere of *Pinus densiflora*

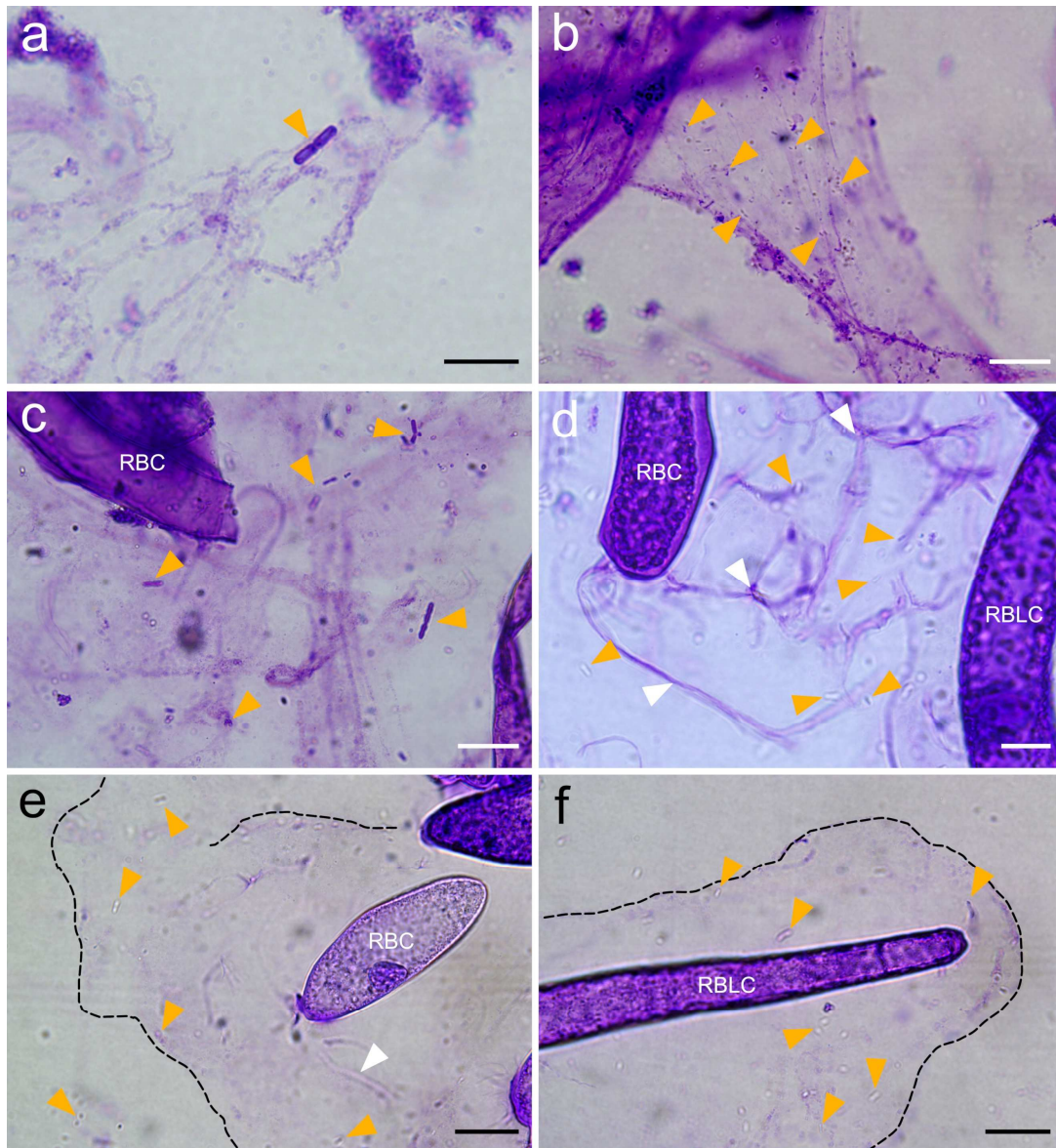
Strain	Abbreviation	Isolation source (location)	Accession no.	Top BLAST hit in GenBank (acc. no.)	Similarity (%)
<i>Bacillus</i> sp. strain O-EM7	BC O-EM7	ECM root tips (Ome, Tokyo)	LC743733	<i>Bacillus cereus</i> strain CASMBAUDAL1 (KM524118)	99.58
<i>Paraburkholderia</i> sp. strain O-EM8	PM O-EM8	ECM root tips (Ome, Tokyo)	LC743734	<i>Paraburkholderia metrosideri</i> strain 17G39-22 (MH934925)	100
<i>Paraburkholderia</i> sp. strain O-NM9	PS O-NM9	NM root tips (Ome, Tokyo)	LC743735	<i>Paraburkholderia sediminicola</i> strain HU2-65W (MN727305)	99.18
<i>Paraburkholderia</i> sp. strain T-NM22	PF T-NM22	NM root tips (Tanashi, Tokyo)	LC743736	<i>Paraburkholderia</i> sp. JSA6 (LC682224)	99.66

ECM, ectomycorrhizal; NM, non-mycorrhizal

612  
613  
614  
615  
616  
617  
618  
619  
620  
621  
622  
623  
624  
625  
626  
627  
628  
629  
630  
631  
632  
633  
634  
635  
636



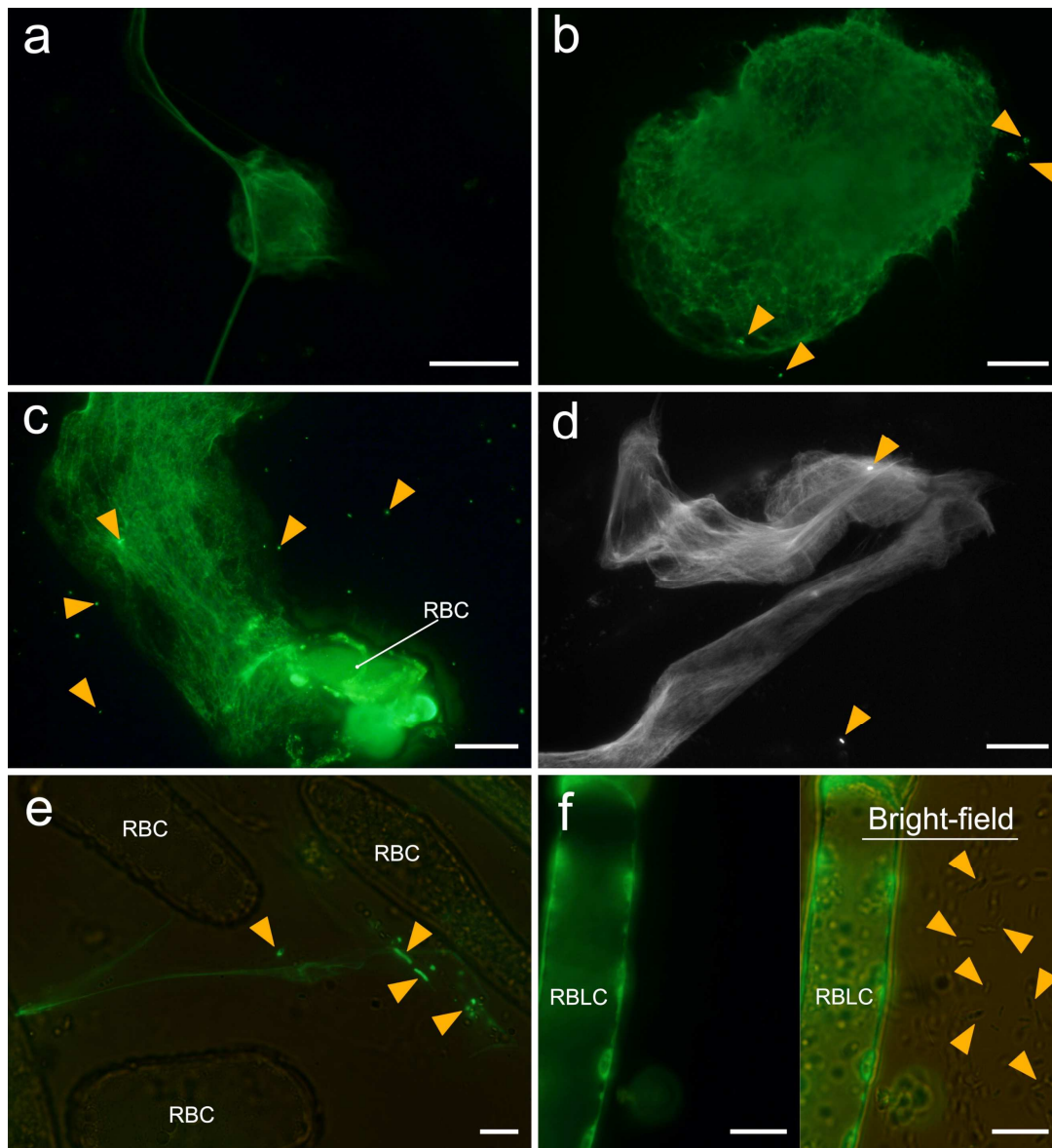
637 **Fig. 1** Histological and histochemical imaging of the main components of the root extracellular traps in the  
638 early growth stage of *Pinus densiflora*. **a, b** A root tip after swelling treatment. **c** A root cap and root-  
639 associated, cap-derived cells (AC-DCs). **d** Cell viability of AC-DCs after detachment from the root cap. **e, f**  
640 Root mucilage secretions stained with India ink (**e**) and crystal violet (**f**) solutions. **g-i** Branched strands  
641 protruding from dead (**g**) and living (**h, i**) cells. **j, k** Merged images of actin filaments (gray) and nuclei (blue)  
642 in AC-DCs. **l** Nuclei of dead cells and strands protruding from cells. **m-o** Extracellular DNA spread in a  
643 thread-like or web-like structure. The abbreviations in the upper right corner of each image indicate the  
644 staining solutions applied: FDA, fluorescein diacetate solution; II, India ink; CV, crystal violet; CW, calcofluor  
645 white; Ph, Acti-stain 555 fluorescent phalloidin; DAPI, 4',6-diamidino-2-phenylindole; and Sg, SYTOX  
646 Green. White arrowheads point to branched strands. The images in **c** and **l** were adjusted for brightness and  
647 contrast using GIMP. Bars: **a** = 5 mm; **b** = 1 mm; **c** = 200  $\mu$ m; **d** (lower right), **e** = 100  $\mu$ m; **n** = 50  $\mu$ m; **d**  
648 (lower left), **f, h-j, l, m, o** = 20  $\mu$ m; **g, k** = 10  $\mu$ m



649

650 **Fig. 2** Trapping of rhizobacteria by root mucilage secretions. The primary root and bacterial strains were co-  
 651 incubated at 25°C for 8 h (**a, b**) or 2 days (**c–f**). Staining with crystal violet solution revealed the results of co-  
 652 incubation with **a, c** *Bacillus* sp. strain O-EM7 and **b, d–f** *Paraburkholderia* sp. strain O-NM9. RBC, root  
 653 border cell; RBLC, root border-like cell. White and yellow arrowheads point to branched strands and bacterial  
 654 cells, respectively. The black dashed lines in **e, f** denote the boundaries of the root mucilage. The images in **a**,  
 655 **d–f** were adjusted for brightness and contrast using GIMP. Bars: **b, c, e, f** = 20 µm; **d** = 10 µm; **a** = 5 µm

656



657

658 **Fig. 3** Visualization of the unfolding of extracellular DNA and subsequent trapping of rhizobacteria. The  
 659 primary root of *Pinus densiflora* and bacterial strains were co-incubated at 25°C for 8 h (a) or 2 days (b–f).  
 660 Staining with SYTOX Green revealed the results of co-incubation with a *Paraburkholderia* sp. strain O-EM8;  
 661 b, e *Bacillus* sp. strain O-EM7; and c, d, f *Paraburkholderia* sp. strain O-NM9. Yellow arrowheads point to  
 662 dead (a–e) and live (f) bacterial cells. Bars: a, c = 50 μm; b, d = 20 μm; e, f = 10 μm

663

664

665  
666  
667  
668  
669  
670  
671  
672  
673  
674  
675  
676  
677  
678  
679  
680  
681  
682  
683  
684  
685  
686  
687  
688  
689

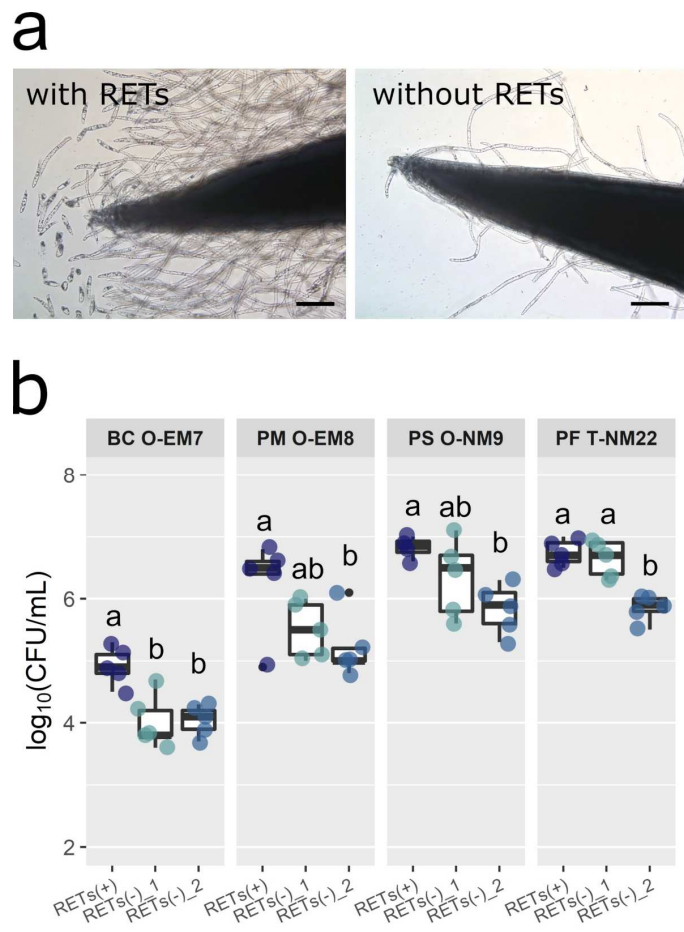


**Fig. 4 a** Primary root tip of *Pinus densiflora* before and after the root extracellular traps (RETs) were removed.  
**b** Colony forming units in the rhizosphere of *P. densiflora* after 2 days of co-incubation with the rhizobacterial strains (n = 5) *Bacillus* sp. strain O-EM7 (BC O-EM7), *Paraburkholderia* sp. strain O-EM8 (PM O-EM8), *Paraburkholderia* sp. strain O-NM9 (PS O-NM9), and *Paraburkholderia* sp. strain T-NM22 (PF T-NM22). In **b**, three treatments are compared: RETs (+), control treatment (no RET removal); RETs (-)\_1, removal of RETs before the co-incubation; and RETs (-)\_2, removal of RETs after the co-incubation. Different letters (a, b) indicate significant (p < 0.05) differences among the treatments according to Tukey's HSD test

690  
691  
692  
693  
694  
695  
696  
697  
698  
699  
700  
701  
702  
703  
704  
705  
706  
707  
708  
709  
710  
711  
712  
713  
714  
715

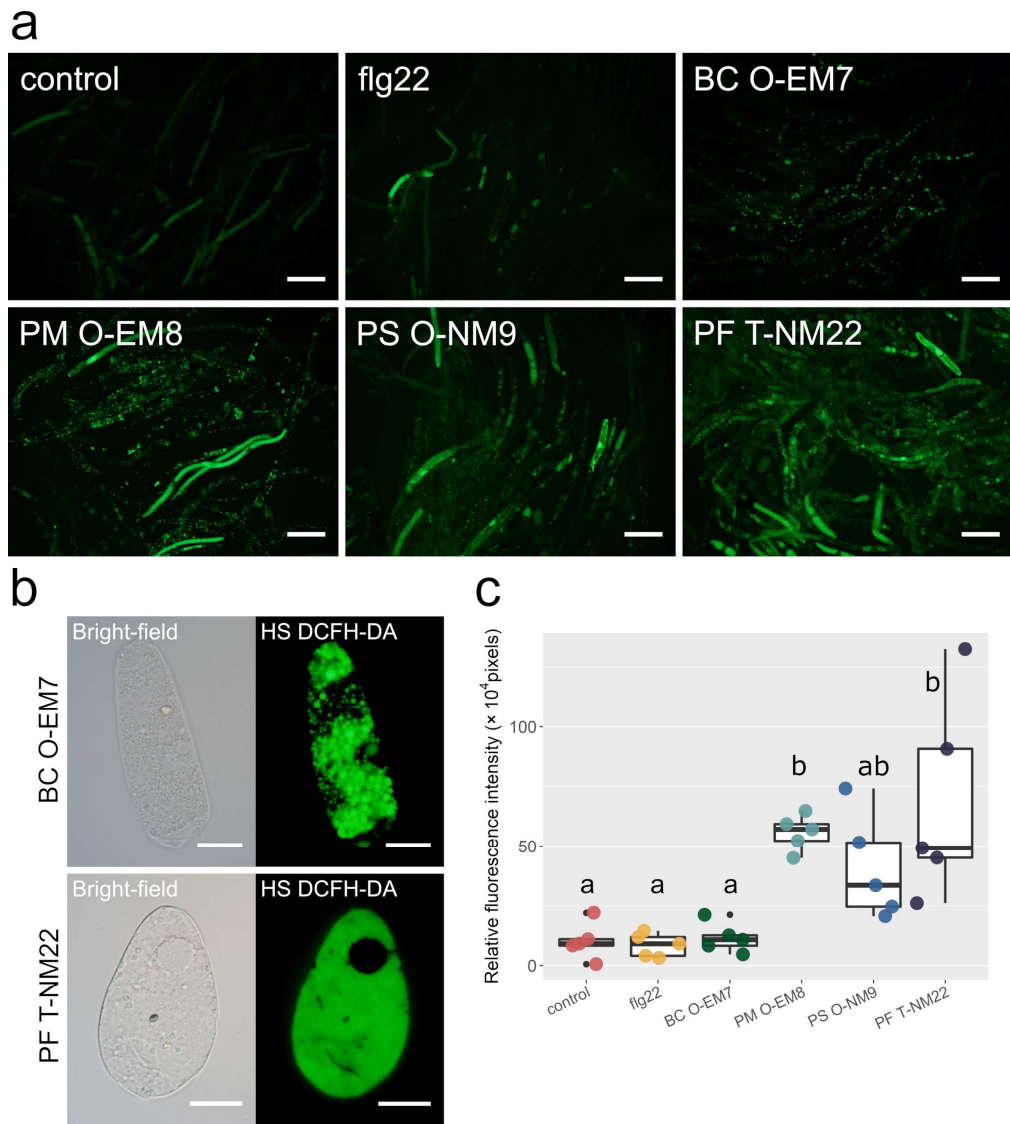


**Fig. 5 a** Production of reactive oxygen species (ROS) in root-associated, cap-derived cells (AC-DCs) from *Pinus densiflora* in the early growth stage after various treatments: Control, no treatment; flg22, incubation with the peptide flg22; BC O-EM7, incubation with *Bacillus* sp. strain O-EM7; PM O-EM8, incubation with *Paraburkholderia* sp. strain O-EM8; PS O-NM9, incubation with *Paraburkholderia* sp. strain O-NM9; PF T-NM22, incubation with *Paraburkholderia* sp. strain T-NM22. Bars = 100  $\mu$ m. **b** Fluorescent patterns of root border cells that showed ROS bursts, detected using the fluorescent probe ROS Assay Kit – Highly Sensitive DCFH-DA (HS DCFH-DA). Bars = 20  $\mu$ m. **c** Relative fluorescence intensity of total ROS in the AC-DCs from the early growth stage of *P. densiflora* in response to inoculation of each bacterial strain (n = 5). Different letters (a, b) indicate significant (p < 0.05) differences among the treatments and bacterial strains, according to Tukey’s HSD test

716

717

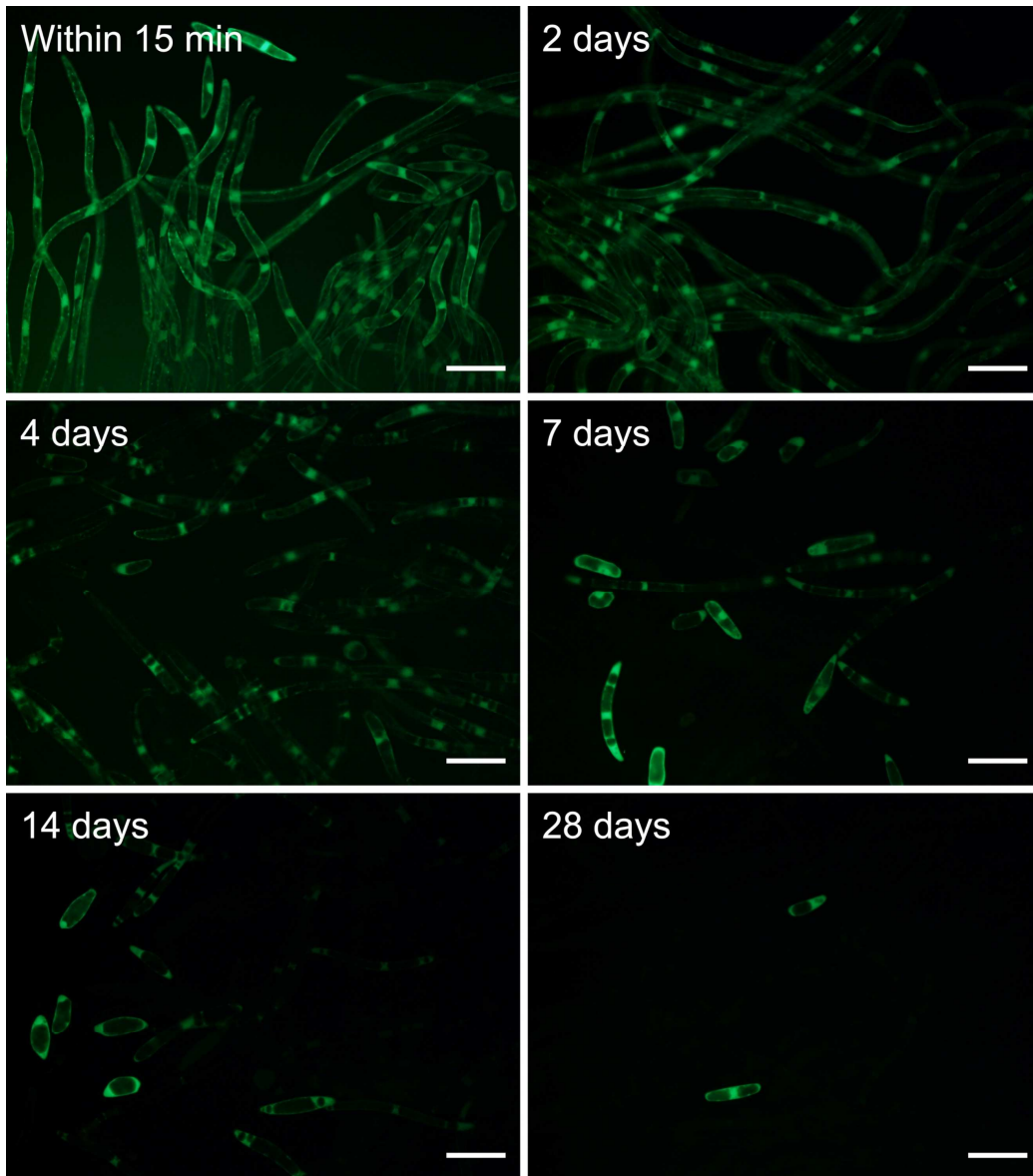
718

719

720

721

722



723

724

725

726

727

728

729

730

731

732

733

734

735 **Fig. S1** Cell viability of root-associated, cap-derived cells (AC-DCs) from the early growth stage  
736 of *Pinus densiflora*. AC-DCs separated from the root cap were incubated in a 1.5 mL tube  
737 containing 200 μL sterile water at 25°C within 15 min and for 2, 4, 7, 14, and 28 days. To  
738 identify live versus dead cells, we used fluorescein diacetate solution ( $1 \mu\text{g}\cdot\text{mL}^{-1}$  in phosphate-  
739 buffered saline) and 0.01% (v/v) Evans blue solution. Bars = 100 μm

740

741

742 **Captions for Online Resources** ※ Not available in the preprint version  
743  
744 The Online Resources (movies) were adjusted only for brightness and contrast using DaVinci Resolve  
745 ver. 18.1.2 (<https://www.blackmagicdesign.com/products/davinciresolve/>), except for Online Resource 1  
746  
747 **Online Resource 1**  
748 Release of root border cells from the root cap and expansion of root border-like cell in response to  
749 affusion (sterile water)  
750  
751 **Online Resource 2**  
752 Dispersion of root-associated, cap-derived cells and mucilage secretion in India ink solution  
753  
754 **Online Resource 3**  
755 Cytoplasmic streaming of root-associated, cap-derived cells immediately after the detachment  
756  
757 **Online Resource 4**  
758 Cytoplasmic streaming of root-associated, cap-derived cells after 7 days of incubation (part 1)  
759  
760 **Online Resource 5**  
761 Cytoplasmic streaming of root-associated, cap-derived cells after 7 days of incubation (part 2)  
762  
763 **Online Resource 6**  
764 Root mucilage encompassing the root-associated, cap-derived cells, with adhered rhizobacterial cells  
765 (*Bacillus* sp. strain O-EM7)  
766  
767 **Online Resource 7**  
768 Root mucilage encompassing the root-associated, cap-derived cells, with adhered rhizobacterial cells  
769 (*Paraburkholderia* sp. strain O-NM9) (part 1)  
770  
771 **Online Resource 8**  
772 Root mucilage encompassing the root-associated, cap-derived cells, with adhered rhizobacterial cells  
773 (*Paraburkholderia* sp. strain O-NM9) (part 2)  
774  
775